Towards a new approach in chiral resolution: pressurized-CO_2 assisted preferential cocrystallization

Joséphine de Meester[a], Patrick Layrisse[b], Mathieu Marchivie[c], Laurent Collard[a], Guillaume Wery[a], Clément Brandel[d], Yohann Cartigny[d], Pascale Subra-Paternault[b], Tom Leyssens[a], Christelle Harscoat-Schiavo[b*]

[a.] Institute of Condensed Matter and Nanosciences, UCLouvain, Place Louis Pasteur 1, 1348 Louvain-la-Neuve, Belgium

[b.] Univ. Bordeaux, CNRS, Bordeaux INP, CBMN, UMR 5248, F-33600 Pessac, France

[c.] Univ. Bordeaux, CNRS, Bordeaux INP, ICMCB, UMR 5026, F-33600 Pessac, France

[d.] Laboratoire Sciences et Méthodes Séparatives, Université Rouen Normandie, Place Emile Blondel, 76130, Mont-Saint-Aignan, France

* christelle.harscoat-schiavo@u-bordeaux.fr

Abstract

We here report the first occurrence of a preferential cocrystallization process assisted by compressed carbon dioxide. Our study focuses on the Nefiracetam-Mandelic acid conglomerate forming system. The cocrystal conglomerate was successfully crystallized using compressed CO_2 as antisolvent, and acetone, ethyl acetate, or isobutanol as solvents for starting solutions in the so-called GAS process. We then focus on acetone to successfully perform preferential cocrystallization supported by compressed CO_2. A critical step in the design of the process is the adaptation of the set-up to allow the introduction of enantiopure seeding inside the reactor. Based on the use of seeded rings, we test several seeding

Abbreviations: GAS, gaseous anti solvent; SC-CO_2, supercritical CO_2; *ee*, enantiomeric excess; nefi, nefiracetam; MA, mandelic acid; EtOAc, ethyl acetate.

configurations to enhance enantioseparation through the simultaneous crystallization of both enantiomers in two different areas of the reactor.

Keywords

Cocrystal, Conglomerate, Preferential crystallization, Antisolvent, CO_2, Seeding

1. Introduction

Chirality, the property of molecules to exist in distinguishable mirror-image forms, plays a pivotal role across various industries, including agrochemical, food, pharmaceutical, material, …[1–4]. The demand for enantiopure compounds arises from the distinct physicochemical properties exhibited by enantiomers in asymmetric environments, such as the human body [1–3]. Consequently, extensive research efforts are focused on developing methods for the production of enantiopure molecules. These processes can be roughly divided into two categories: asymmetric synthesis and chiral resolution. In asymmetric synthesis, the aim is to selectively synthesize the desired enantiomer [1,2], whereas for resolution methodologies, racemic mixtures are produced, and enantiomers are subsequently separated using a physical separation technique [1,5]. Various methods of chiral resolution have been developed over the recent decades, one of which is preferential crystallization [1,5,6].

Preferential crystallization is a kinetic process that relies on a difference in crystallization rate of enantiomers through the use of homochiral seeds. The technique requires the compound to crystallize as a conglomerate – a physical mixture of enantiopure crystals [6]. This forms a major limitation to the methodology, as a mere 5 to 10% of chiral molecules crystallize as a conglomerate [1,5,6]. To broaden the scope of this technique, ongoing research endeavors aim to convert racemic compounds – containing equal amounts of both enantiomers in the crystal unit cell – into conglomerates. Various crystal engineering strategies [7] have been applied in this context over the recent years including salt [8,9], solvate [10], and cocrystal [5,11–14] formation. As an example, Buol et al [5], illustrated the cocrystal approach, transforming the racemic compound mandelic acid (MA) into a conglomerate through a (1:1) cocrystallization with nefiracetam (nefi) (Figure 1). They furthermore used this finding to develop a resolution through preferential cocrystallization, working with acetonitrile.

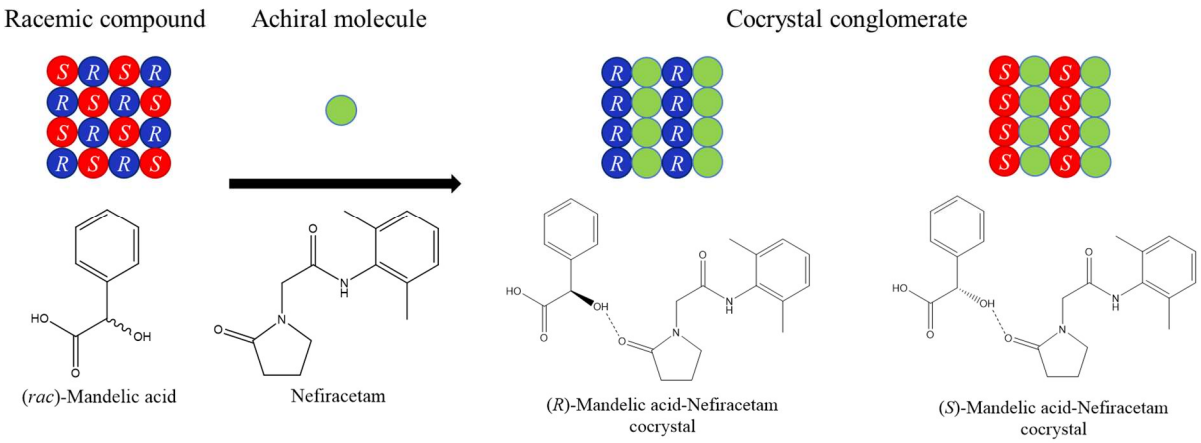

Figure 1. Conversion of the racemic compound mandelic acid into a conglomerate through cocrystallization with nefiracetam.

In this work, we want to take this system one step further. We pioneer in showing how pressurized carbon dioxide can be successfully used in the context of preferential crystallization.

The recent increase in pressurized carbon dioxide, and particularly supercritical carbon dioxide (SC-CO_2), research reflects the growing interest in this fluid. Indeed, SC-CO_2 is considered as non-toxic, non-flammable, chemically inert, and is recyclable through pressure reduction [4,15–18].

The versatility of SC-CO_2 spans various processes. Its relatively low critical temperature (31°C) allows the extraction of thermally unstable compounds. Moreover, it serves as a solvent for various reactions [16,19], or even as an antisolvent for particle micronization [20,21] and cocrystallization [22–25]. Furthermore, SC-CO_2 finds applications in polymer synthesis, and textile dyeing [21].

This study contributes to the continuous expanding field of compressed CO_2 research, by exploring its potential in chiral resolution. While SC-CO_2 processes have already been successfully studied in the context of diastereomeric salt resolution [15,26–29], here we broaden the scope by showcasing the feasibility to develop preferential cocrystallization assisted by pressurized CO_2. We do so, focusing on the chiral resolution of the nefi-MA cocrystal, using CO_2 as an antisolvent. We began by exploring the ability of SC-CO_2 to induce conglomerate cocrystal formation, to then develop a preferential crystallization process assisted by CO_2. With our study, we lay the next brick for the consolidation of CO_2 processes as alternative tools for chiral resolution.

2. Materials and methods

2.1. Materials

Nefiracetam (LSherb), (*rac*)-mandelic acid (TCI Chemicals), (*R*)-mandelic acid (TCI Chemicals), (*S*)-mandelic acid (TCI Chemicals), acetone (HPLC grade, Atlantic labo), ethyl acetate (EtOAc, analytical grade, Atlantic labo), isobutanol (analytical grade, Atlantic labo), isohexane (analytical grade, Atlantic labo), absolute ethanol (Atlantic labo) , 2-propanol (Atlantic labo), trifluoroacetic acid (Atlantic labo), phosphoric acid (Atlantic Labo), acetonitrile (HPLC grade, Atlantic labo) and carbon dioxide (CO_2, 99.5%, Messer) were purchased from commercial sources and used as such.

For convenience, nefiracetam will be abbreviated as nefi, and mandelic acid as MA throughout the rest of the document.

2.2. Enantiopure seed preparation

Enantiopure seeds were obtained on larger scale (approximately 20 g) from ethyl acetate. Equimolar amounts of nefiracetam (15.00 g) and (*R*)-MA or alternatively (*S*)-MA (9.27 g) were introduced in a reactor vessel filled with ethyl acetate (100 mL). The suspension was stirred at 300 rpm for 48 h at RT. Subsequently, the suspension was filtered and the resulting powder was washed with ethyl acetate and dried. This material served as the seeding material for preferential crystallization experiments.

2.3. X-ray powder diffraction (XRPD)

Two instruments were used for the XRPD data collection.

Part of the samples were measured using a Siemens D5000 diffractometer equipped with a Cu X-ray source operating at 40 kV and 40 mA. The instrument uses a secondary monochromator to select the Kα radiation of Cu (λ = 1.5418 Å). A scanning range of 2θ values spanned from 5° to 35°.

Alternatively, XRPD data were collected using a PANalytical X'pert PRO MPD diffractometrer equipped with a secondary monochromator and X′Celerator multi-strip detector with copper radiation (λ = 1.5418 Å). A scanning range of 2θ values spanned from 4° to 38°.

The samples were gently ground to limit preferred orientations. The powders were then placed uniformly on sample holders made of aluminium alloy and flattened with a razor blade.

2.4. Chiral High-Performance Liquid Chromatography (*c*HPLC)

Chiral HPLC was used to determine the relative amount of both enantiomers of mandelic acid. Samples were prepared by dissolving the sample in a solution composed of 80 vol.% isohexane, 20 vol.% EtOH. Two instruments were used for chiral high-performance liquid chromatography (*c*HPLC).

Part of the analyses were carried out using a Waters Alliance 2695 coupled with a Waters 996 Photodiode Array Detector (PDA) (λ = 220nm). The column used was a Daicel Chiralpak IC, 4.6 × 250 mm, 5 µm, the sample injection volume was 10 µL. A mobile phase consisting of 95 vol.% isohexane, 5 vol.% 2-propanol, 0.1 vol.% trifluoroacetic acid was used. The separation was achieved in 30 min, at RT with a flow rate of 1 mL/min. After three sample runs, the column was washed with isohexane/ethanol (80/20, v/v) at a rate of 1 mL/min for 30 min.

Alternatively, enantiomeric quantification was performed using an Agilent Infinity 1260 system (Agilent Technologies) equipped with a degasser, a quaternary pump, an automatic injector, a diode array detector (DAD) and Chemstation software for data acquisition. The column and method used were identical to the procedure described above.

Each data point is the average of two distinct samples of 20 mg powder in 20 mL solution.

Enantiomeric excess was calculated for each sample. It is used to express the excess of one enantiomer over the second in a mixture. The formula used is as follows:

$$ee\ (\%) = \frac{\big((R) - \text{enantiomer}\big) - \big((S) - \text{enantiomer}\big)}{\big((R) - \text{enantiomer}\big) + \big((S) - \text{enantiomer}\big)} \text{x } 100$$

A compound with an enantiomeric excess of 0% is racemic, while when the enantiomeric excess is 100%, the compound is enantiopure.

2.5. Reverse High-Performance Liquid Chromatography (*r*HPLC)

Reverse HPLC is used to quantify exact amounts of nefiracetam vs mandelic acid. The compounds were dissolved in a solution composed by 50 vol.% acetonitrile, 50 vol.% Milli-Q water. Calibration curves for reverse high-performance liquid chromatography (*r*HPLC) were built correlating the area under the curve (AUC) with the concentration used following a linear equation. Calibration lines (at $\lambda = 210$ nm) are reported in Figures SI-1 and SI-2.

For dosing nefi:MA molar ratios, samples were prepared by dissolving the sample in a solution composed by 50 vol.% acetonitrile, 50 vol.% Milli-Q water. The instrument used was an Agilent Infinity 1260 system (Agilent Technologies) equipped with a degasser, a quaternary pump, an automatic injector, a diode array detector (DAD) ($\lambda = 210$nm) and Chemstation software for data acquisition. The column used was a Kinetex C18 F5 (Phenomenex), 100x4.6 cm, 2.6 μm, the sample injection volume was 5 μL. The separation, performed at 40 °C with a flow rate of 1 mL/min, was achieved in 14 min. The mobile phase consisted of a gradient of solution A – water + 0.1 vol.% phosphoric acid (H_3PO_4) and solution B – acetonitrile + 0.1 vol.% H_3PO_4 in the following sequence: 0 to 0.5 min at 30% B, followed by increasing B from 30% to 90% in 5 min, a step of 1 min at 90% B and reequilibration at 30% B during the remaining 7.5 min.

Each data point is the average of two distinct samples of 10 mg powder in 20 mL solution.

2.6. Cocrystallization using CO_2 as an antisolvent

The experimental set-up used is a custom-built Gaseous Anti Solvent (GAS) equipment (Scheme 1). The process starts by loading the pre-heated reactor with a volume of solution and subsequently introducing CO_2. Nefi and MA were dissolved in 30 mL of acetone, EtOAc or isobutanol at various concentrations and molar ratios. The solution was placed in an ultrasonic bath for approximately 3 minutes to ensure complete dissolution of all starting materials, then it was pre-heated on a hot plate. The 0.49 L reactor is equipped with three sapphire windows, and a stainless-steel filter topped with a 0.2 μm pore size membrane at its bottom. A mechanical stirrer ending with a hollow Rushton turbine plunged into the solution and allowed direct dispersion of the CO_2 into the solution. The stirring rate

was set to 300 rpm. A glass cylinder covering the inner surface of the reactor was used for easy recovery of the crystals obtained. The reactor temperature (40 °C) was regulated by a heating tape and monitored by a sensor centrally positioned about 2 cm above the Rushton turbine. Compressed CO_2 was first cooled in a cryostat at 0 °C and its introduction was carried out using an SFE (Model HPP400-B, SFE Process) pump at a rate of 11 g/min. During this step, as CO_2 was added gradually, the pressure inside the vessel increased and the solvent-CO_2 mixture shifted from a liquid-vapor system to a monophasic fluid. At the same time, the solubility of components decreased, leading to a precipitation event that could be observed through the sapphire windows. Once the desired pressure of 10.0 MPa was reached, the formed CO_2-solvent mixture was drawn from the bottom of the reactor while fresh CO_2 was added to the system at 35 g/min to maintain the pressure and to dry the obtained powder. The pressure in the reactor was controlled at 10.0 ± 0.5 MPa by an exit metering valve. At the end of the process, the system was depressurized through the exit line, and particles were collected, weighed and analyzed.

The resulting powder was collected in different fractions: on the stirrer shaft, inside the reactor, and inside the outlet collector.

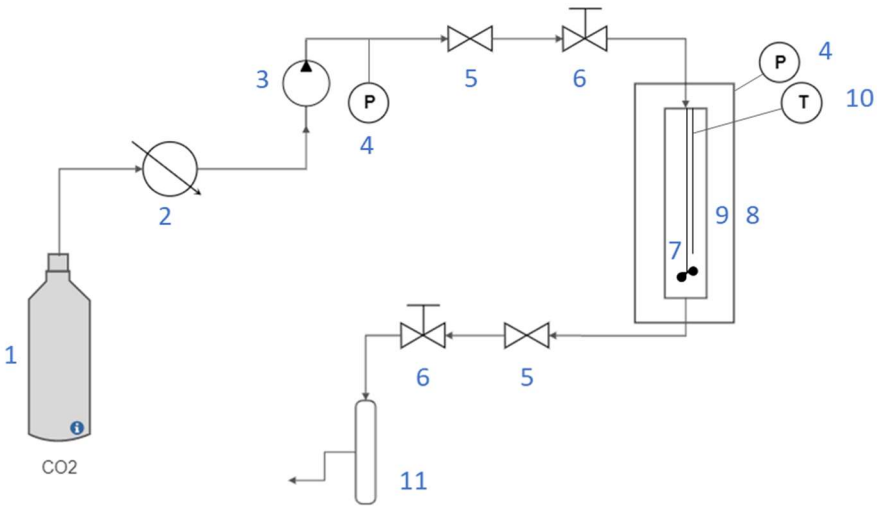

Scheme 1. GAS set-up, with 1. CO_2 tank; 2. cooler; 3. CO_2 pump; 4. pressure gauge; 5. valve; 6. metering valve; 7. mechanical stirrer; 8. reactor; 9. glass cylinder; 10. thermocouple; 11. outlet collector.

2.7. Preferential cocrystallization using a CO_2 antisolvent process

The method and instrumentation used are identical to the one described in Section 2.6 (Cocrystallization using CO_2 as an antisolvent), with exception of the moment the solution was withdrawn from the vessel. The process was halted when the experimenter observed the solution to become turbid, which occurred at different pressures for each experiment. As preferential crystallization requires seeding, an enantiopure seeding set-up was used to guide the outcome of the process. Seeding material was added on the inner face of the glass cylinder, above the solution level, at a height of 4.5-5.5 cm. To do this, enantiopure seed was slurried in acetone, the slurry was subsequently applied on the surface of the cylinder and acetone was allowed to evaporate, leaving a solid enantiopure crust on the cylinder. Initial experiments used a one-piece cylinder. Subsequently, a transition was made to a cylinder composed of three parts (respectively of 4.5 cm – 1 cm – 16.5 cm) to facilitate the seeding process, and the collection of crystals after the experiment.

Upon completion of the process, the resulting powder was collected in the various parts of the reactor: on the stirrer shaft, on the seeded cylinder (powder crystallizing on the enantiopure seeds), inside the reactor (remaining powder inside the reactor), and inside the outlet collector. Prior to powder collection on the seeded cylinder, meticulous sampling was performed on both the outer surface and deeper inside the layer, closer to the seed, utilizing a thin spatula. To do this, we first collected a small amount of surface powder, and then dug for collecting powder at greater depth.

3. Results and discussions

3.1 Enabling the conglomerate cocrystallization process

First, our investigation focused on the feasibility of forming the nefi-MA cocrystal using a CO_2 antisolvent process. Initial attempts aimed at selecting a solvent. To achieve this, (1:1) stoichiometric ratios of nefi and enantiopure or racemic MA were dissolved in ethyl acetate (EtOAc), acetone, or isobutanol (Table 1). CO_2 was introduced until achievement of a final pressure of 10 MPa. In all experiments, the mixture became turbid before reaching this pressure. This shows that crystallization had occurred prior to reaching 10 MPa and that CO_2 effectively acts as an antisolvent in this process.

All experiments led to the formation of the cocrystal (Figure 2). Moreover, experiments involving enantiopure mandelic acid (Runs 1-3), led to the crystallization of pure cocrystal material, as confirmed by XRPD (Figure 2) and *r*HPLC (Table 1). With racemic mandelic acid, however, experiments resulted in cocrystal formation combined with concomitant crystallization of the nefi parent compound for all of the three solvents used (Runs 4-6, Figure 2), indicating the need to adapt the nefi:(*rac*)-MA ratio in these solvents. When using EtOAc or acetone, *r*HPLC data aligns with XRPD results, confirming the slight excess of nefi in the obtained powders, while with isobutanol, the excess of nefi is only observable with XRPD analysis. The low *ee*'s obtained when starting from racemic mandelic acid fall within experimental error, and indicate that chiral resolution did not occur spontaneously. This is expected as both enantiomeric cocrystals show identical crystallization kinetics in the absence of a chiral external factor. As in classical preferential crystallization processes, enantiopure seeding is a necessity to promote selective growth of a given enantiomer [6].

Table 1. Cocrystallization experiments of nefi and MA by GAS in EtOAc, acetone, and isobutanol.

Run	Initial compounds	Solvent	C(nefi + MA) (g/L)	Crystallization yield* (%)	Product	Nefi:MA molar ratio of the recovered powder**	*ee* reactor***
1	nefi + (*S*)-MA (1:1)	EtOAc	48.4	63.3	nefi-(*S*)-MA cocrystal	(1:1)	-
2	nefi + (*S*)-MA (1:1)	Acetone	66.4	64.6	nefi-(*S*)-MA cocrystal	(1:1)	-
3	nefi + (*S*)-MA (1:1)	Isobutanol	66.4	28.5	nefi-(*S*)-MA cocrystal	(1:1)	-
4	nefi + (*rac*)-MA (1:1)	EtOAc	48.4	64.0	nefi-(*rac*)-MA cocrystal + nefi	(1.1:1)	-2
5	nefi + (*rac*)-MA (1:1)	Acetone	66.4	48.8	nefi-(*rac*)-MA cocrystal + nefi	(1.1:1)	0

6	nefi + (*rac*)-MA (1:1)	Isobutanol	66.4	22.1	nefi-(*rac*)-MA cocrystal****	(1:1)****	0

*The crystallization yield was determined as the amount recovered on the stirrer shaft, and inside the reactor at the end of the experiment compared to the total amount of material used. Remaining powder was found in the outlet collector.

**Nefi:MA molar ratios of the obtained products were determined by *r*HPLC.

****ee* were determined by *c*HPLC.

****Traces of nefi are observed by XRPD.

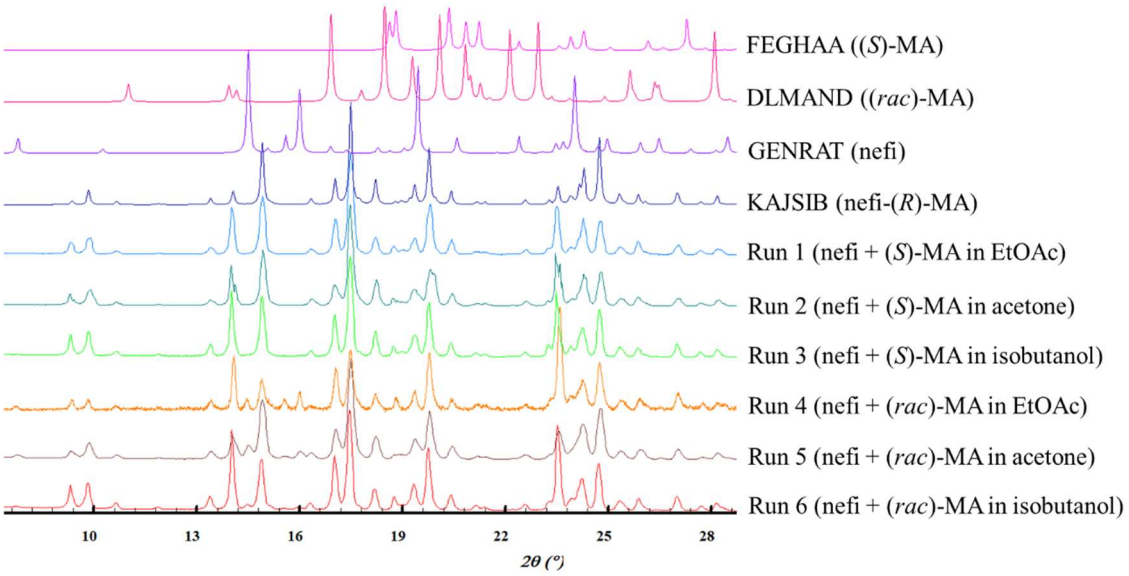

Figure 2. Comparison of the XRPD patterns of nefi-(*rac*)-MA (1:1) cocrystallization through GAS in isobutanol (red), acetone (brown), EtOAc (orange), nefi-(*S*)-MA (1:1) cocrystallization through GAS in isobutanol (light green), acetone (dark green), and EtOAc (light blue), and the simulated patterns of the reported nefi-(*R*)-MA-cocrystal (CCDC refcode KAJSIB) [5] (dark blue) and parent compounds nefi (CCDC refcode GENRAT) [30] (violet), (*rac*)-MA (CCDC refcode DLMAND) [31] (magenta), and (*S*)-MA (CCDC refcode FEGHAA) [32] (pink).

Overall, these results show that any of the three solvents above can be successfully used to crystallize both enantiopure, and the conglomerate cocrystal using SC-CO_2 technology. We then moved to the next step, being the development of a preferential crystallization process.

3.2 Preferential crystallization

3.2.1 *Process design*

Even though all three solvents seemed appropriate, acetone was selected for the remainder of the study, based on our expertise with this solvent in the frame of crystallization using CO_2 as an antisolvent [22,23,33,34]. As starting from (*rac*)-MA, some amount of nefiracetam crystallizes together with the cocrystal conglomerate, experiments were performed adjusting the nefi:(*rac*)-MA molar ratio (Table 2, Runs 7-11). As confirmed by XRPD and *r*HPLC analysis, decreasing the ratio to (0.7:1) resulted in the production of pure cocrystal material. This optimized ratio was used in all subsequent resolution experiments.

As mentioned above (Runs 4-6), and as expected, processes performed without enantiopure seeding always resulted in the crystallization of both enantiomers. To incorporate seeding in a CO_2 antisolvent process, we designed a set-up wherein a cylinder is coated with seed material at a given height (Figure 3a). To prevent these seeds from dissolving in contact with the solution initially introduced, this seed material is set above the solution level (Figure 3b, t_0). Upon CO_2 introduction, as CO_2 is miscible with the used solvent, the solution expands while the solubility of the compounds in the newly expanded CO_2-solvent solution decreases. The solution should become supersaturated prior to reaching the seed material. Upon reaching this latter (Figure 3b, t_f), preferential growth can theoretically be initiated on the seeded cylinder (Figure 3c). The seeding height, therefore, needs to be carefully controlled, depending both on the nature of the solvent as well as the overall concentration. If the seed material is reached too rapidly, the overall solution might still be undersaturated and the seeds would dissolve. If the seed coating is positioned too high, spontaneous concomitant crystallization of both enantiomers from a highly supersaturated solution occurs prior to reaching the seed material. In our set-up, a 1 cm seeded coating ring was always placed at a height of 4.5-5.5 cm.

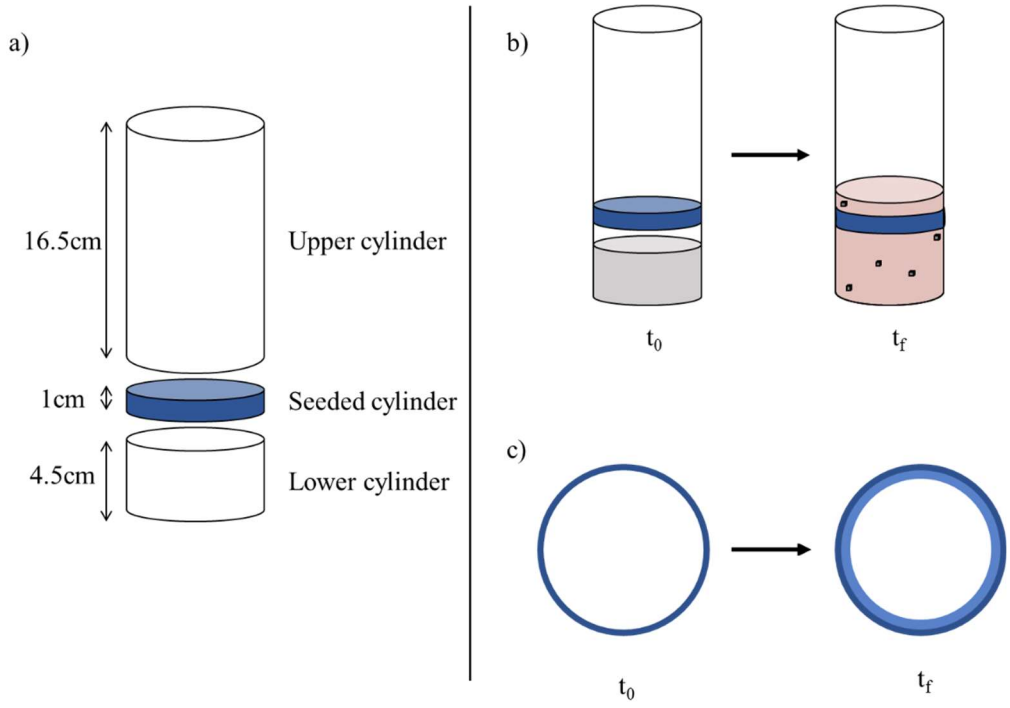

Figure 3. Preferential crystallization principle. a) Set-up of the cylinder, with the seed material at a height of 4.5-5.5 cm, b) Evolution of the experiment over time, with the racemic initial solution in grey and the final solution, enriched in counter-enantiomer, in pink, c) Schematic theoretical crystal growth on the seeded cylinder at the end of the process, with the seed material in dark blue and the outcome of the crystallization in light blue.

The set-up presented here also requires the establishment of an endpoint. As for all preferential crystallization processes, if supersaturation keeps being increased, the counter-enantiomer will inevitably also crystallize out. In our case, if upon initial crystallization, CO_2 keeps on being injected, the supersaturation of the counter-enantiomer continues to increase until its spontaneous crystallization. It was, therefore, decided to stop the process as soon as turbidity was observed in the reactor through the sapphire windows, for a pressure between 6.6 and 7.2 bar (Table 2). At this stage, if preferential crystallization occurred, an enantiomeric excess in favor of the seed enantiomer should be observable in the recovered powder.[2] Three experiments were stopped while the solution was still limpid, at

[2] Seeding height, and concentrations used are appropriate for acetone. These parameters need to be adapted when using isobutanol or EtOAc.

pressures ranging between 6 and 6.5 bar (Table 2). These indeed showed almost no crystallization occurred within the reactor, and that no additional mass was recovered atop the seeds (Table 2, Runs 12-14), confirming that the onset of turbidity can be taken as the point at which cocrystallization takes place.

As already highlighted by experiments 4-6, resolution does not occur in absence of seeding. This was confirmed, conducting two experiments using non-seeded cylinders (Table 2, Runs 15-16). A first trial was performed using a (1:1) nefi:(*rac*)-MA molar ratio, while for a second experiment, this ratio was adjusted to (0.7:1). Both experiments were stopped when turbidity was observed. As expected, extra nefi was observed in Run 15 by XRPD analysis, while Run 16, with the (0.7:1) adjusted ratio, led to pure cocrystal (Figure SI-3, Table 2). In both cases, racemic mixture material was obtained in all parts of the reactor (stirrer, cylinder, reactor) and outlet collector. These experiments, therefore, once more confirm spontaneous preferential growth of neither nefi-(*R*)-MA nor nefi-(*S*)-MA occurs in any point of the experimental set-up in the absence of seeds. As for solution-based preferential crystallization processes, seeding is also a prerequisite in a pressurized-CO_2 set-up if preferential crystallization is to be induced.

Table 2. GAS-assisted preferential crystallization experiments.

	Run	Nefi : (rac)-MA initial ratio	Initial solution cc. (g/L)		Seeded enantiomer	m_{seed} (mg)	Pressure at flush (MPa)	Crystallization $yield_{tot}$ (%)	Crystallization $yield_{cyl}$ (%)	Nefi:MA molar ratio of the recovered powder *	*ee* cyl** (%)	*ee* stirrer** (%)	*ee* reac** (%)	*ee* coll** (%)
			Nefi	MA										
Adaptation of nefi:MA ratio + Introduction of enantiopure seeding	**7**	(1:1)	41.06	25,31	*R*	548	6.7	33.0	16.7	(1.1:1)	34	-13	-9	---
	8	(0.8:1)	32.80	25,37	*R*	296	6.8	40.1	15.3	(1:1)***	12	-9	-4	-1
	9	(0.8:1)	32.70	25,32	*R*	314	6.9	39.6	18.2	(1.1:1)	15	-20	-10	1
	10	(0.7:1)	28.76	25,43	*R*	279	6.9	35.3	16.1	(1:1)	27	-32	-22	1
	11	(0.7:1)	28.68	25,36	*R*	263	6.6	49.0	12.2	(1:1)	40	-20	-21	4
Process stopped before turbidity	**12**	(0.8:1)	32.62	25.39	*R*	264	6.0	1.9	0	---	---	---	---	---
	13	(0.8:1)	32.75	25.35	*R*	293	6.2	1.9	0	---	---	---	---	---
	14	(0.8:1)	32.76	25.36	*R*	309	6.5	5.9	0	---	---	---	---	---
No seeding	**15**	(1:1)	40.97	25.36	---	---	7.1	56.2	25.3	---	1	0	0	---
	16	(0.7:1)	28.91	25.61	---	---	6.8	46.3	12.5	(1:1)	2	-2	1	1
Decreasing seeds amount	**17**	(0.7:1)	28.87	25.45	*S*	104	6.9	46.8	19.0	(1:1)	-24	26	15	-6
	18	(0.7:1)	28.78	25.40	*R*	3	6.9	52.2	7.6	---	31	-3	-5	0
Decreasing concentration	**19**	(0.7:1)	22.68	20.03	*R*	3	7.2	52.5	7.9	---	44	-20	6	3
	20	(0.7:1)	22.68	20.01	*S*	4	6.9	46.2	13.0	---	-49	25	13	0
	21	(0.7:1)	28.93	25.61	*S*	7	6.9	39.2	9.9	(1:1)***	-37	1	2	0
					R	4			7.3	(1:1)	33			

Simultaneous	**22**	(0.7:1)	28.90	25.58	*S*	2	6.9	27.0	3.9	---	-23	-5	-1	2
seeding of both					*R*	2			5.7	---	24			
enantiomers	**23**	(0.7:1)	28.78	25.38	*S*	3	6.7	41.2	4.2	---	-65	1	5	0
					R	1			4.7	---	34			
	24	(0.7:1)	28.78	25.44	*S*	1	6.9	36.6	6.3	---	-20	-4	-2	1
					R	2			4.8	---	44			
	25	(0.7:1)	28.75	25.47	*R*	3	6.8	48.3	6.0	---	8	-1	2	0
					S	3			2.8	---	-18			
	26	(0.7:1)	28.73	25.41	*R*	4	6.9	50.2	12.4	---	21	2	1	0
					S	5			9.0	---	-38			

*Nefi:MA molar ratios of the obtained products were determined by *r*HPLC.

***ee* were determined by *c*HPLC, a positive result represents an enrichment in nefi-(*R*)-MA, and a negative result represents an enrichment in nefi-(*S*)-MA. The *ee* of the cylinder corresponds to that of the supplementary material that crystallized on top of the seed material. To calculate this *ee*, the seed-mass was subtracted from the total mass recovered, and *r*HPLC and *c*HPLC were used to estimate the *ee* of the supplementary material.

***Traces of nefi are observed by XRPD and a low excess of nefi is observed by *r*HPLC.

3.2.2 *Inducing preferential crystallization*

3.2.2.1. Introduction of enantiopure seeding

A first set of experiments comprising various molar ratios of nefi:MA (Table 2, Runs 7-11) was performed, with the cylinder seeded with nefi-(*R*)-MA. It was confirmed that all experiments resulted in an increase of the mass deposited on the seed material.

The global crystallization yield (crystallization $yield_{tot}$) was calculated for all experiments by summing the mass of crystals recovered on the seeded cylinder, the stirrer shaft, and inside the reactor (this amount was corrected for the amount of seed material initially used) compared to the initial amount of the compounds introduced in the solvent. The remaining mass was always recovered in the outlet reactor as crystalline powder.[3] For Runs 7-11, between a quarter and up to half of the total crystallized powder was found on the seeded cylinder.

XRPD (Figure SI-3) and *r*HPLC measurements confirmed the presence of pure cocrystal formation on the seeded cylinder when using a nefi:MA initial ratio of (0.7:1), while containing some supplementary nefiracetam for the higher stoichiometric ratios. Interestingly, the crystal mass deposited on the seed materials during crystallization was systematically found to have an enantiomeric excess in favor of nefi-(*R*)-MA. This result highlights the first successful occurrence of enantioenrichment induced through CO_2-assisted preferential crystallization. The fact that the material is not enantiopure (with *ee*'s

[3] For example, for Run 7, the mass recovered on the seeded cylinder (0.881 g), the stirrer shaft (0.081 g), and inside the reactor (0.244 g) was corrected for the amount of seed (0.548 g), resulting in a crystallization mass of 0.658 g, while the initial mass of compounds in acetone was 1.991 g. This leads to a crystallization yield of 33.0%. In comparison, the crystallization yield on the seeded cylinder (crystallization $yield_{cyl}$) corresponds to the mass recovered on the seeded cylinder (corrected for the initial seed amount), compared with the maximum amount recoverable. For Run 7, this corresponds to 0.333 g (0.881 g corrected for the seed, which was 0.548 g) compared with 1.991 g, resulting in a 16.7% crystallization yield on the cylinder.

ranging from 12 to 40%), is indicative of the counter-enantiomer also crystallizing at a given moment, as is typically the case in preferential crystallization processes.[4]

Further evidence of preferential crystallization is shown by analyzing the powders recovered in the remaining parts of the set-up. For Runs 7-11, both reactor and stirrer recovered materials are enriched in the opposite enantiomer nefi-(*S*)-MA. This aligns with preferential crystallization principles. As more of the nefi-(*R*)-MA crystallized on the seeded cylinder, the remaining solution is enriched in nefi-(*S*)-MA, resulting in more of this enantiomer crystallizing in the reactor and on the stirrer. At the end of the process, the compound remaining in solution (and recovered in the outlet collector) is a racemic mixture. This behavior is observed across all seeded experiments. Therefore, mass balances can be calculated for all experiments.[5]

Additionally, we were able to orient resolution towards one or the other enantiomer. Runs 17 and 20 indeed show that the use of (*S*)-seeds leads to preferential growth, and hence enantioenrichment, of the seed-ring in nefi-(*S*)-MA while the material recovered on reactor and stirrer becomes enriched in nefi-(*R*)-MA.

---

[4] In their original contribution, Buol et al.[5] limited the crystallization yield of each cycle to 5% to avoid the counter-enantiomer of appearing. To achieve such low yields was impossible using the current set-up, explaining the spontaneous crystallization of the counter-enantiomer at a given stage of our process.

[5] For Run 11, for example, powders collected on the stirrer and in the reactor have a mass of respectively 0.229 g and 0.367 g, with respective *ee* values of -20% (*R*-*S* ratio of 0.40-0.60) and -21% (*R*-*S* ratio of 0.395-0.605). Taken together, these materials result in 0.237 g of nefi-(*R*)-MA and 0.359 g of nefi-(*S*)-MA. The quantity of powder collected on the cylinder is 0.198 g with an *ee* of 40% (*R*-*S* ratio of 0.70-0.30). It corresponds to 0.139 g of nefi-(*R*)-MA and 0.059 g of nefi-(*S*)-MA. The remaining powder is found in the outlet collector and corresponds to a mass of 0.827 g with an *ee* of 4% (*R*-*S* ratio of 0.52-0.48), which corresponds to 0.430 g of nefi-(*R*)-MA and 0.397 g of nefi-(*S*)-MA. In total, the recovered amounts of (*R*)- and (*S*)-cocrystal correspond respectively to 0.805 g and 0.816 g. The material balance is therefore respected, with an error attributed to the recovery of the powder in each part of the set-up.

To gain more insight into the crystallization occurring on the seeded ring, the *ee* of the material that crystallized on the cylinder was examined along its depth (Figure 4). To do this, careful sampling was performed on both the outer surface and deeper inside the layer (so closer to the seed). Table 3 illustrates the gradual and preferential crystal growth phenomena. As the seeded layer is enantiopure – typically nefi-(*R*)-MA in our examples – it is first covered by a growth layer enriched in this enantiomer. As a result, the solution becomes enriched in the counter-enantiomer – nefi-(*S*)-MA –, which crystallizes, more strongly, in the outer layers. Table 3 shows that the outer surface, indeed, always exhibits an increased amount of counter-enantiomer compared to the inner layers. In some scenarios (Table 3, Run 10 A and B, Run 11 A and C), the outer layer is even favored with respect to the counter-enantiomer. It should however be noted that the overall *ee* of the cylinder material remains enriched in nefi-(*R*)-MA used as seed. For the samples taken across the crystallized material (designated as A, B, C and D), only a few milligrams of powder were taken each time. Considering the inhomogeneity of the newly crystallized layer and given that sampling along the depth of the seed-cylinder is tedious and not evident, Table 3 shows overall behavior rather than exact *ee*'s.

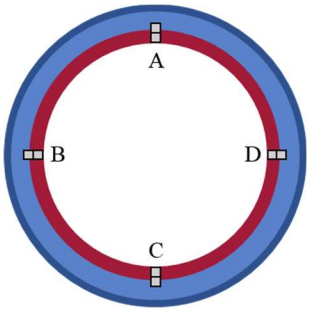

Figure 4. Crystal growth occurs in layers on the seeded cylinder. As one moves away from the initial seed layer to the outer surface, the enrichment in nefi-(*R*)-MA becomes less pronounced. In dark blue, enantiopure seeding, *e.g.* nefi-(*R*)-MA; in light blue crystalline material still enriched in nefi-(*R*)-MA; in dark red, crystalline material enriched in counter-enantiomer, nefi-(*S*)-MA. The different samples taken are represented as grey squares.

Table 3. *c*HPLC results of the samples taken across the crystallized material on the cylinder for Runs 10 and 11. Samples are recovered on outer layer, as well as closer to the surface of the cylinder (inner).

Run	*ee* cyl (%)	*ee* A		*ee* B		*ee* C		*ee* D	
		Outer	Inner	Outer	Inner	Outer	Inner	Outer	Inner
10	27	-24	-11	-25	-17	12	16	13	30
11	40	-1	16	16	31	-1	13	12	9

**ee* were determined by *c*HPLC, a positive result represents an enrichment in nefi-(*R*)-MA, and a negative result represents an enrichment in nefi-(*S*)-MA.

These observations suggest a rapid and preferential growth of nefi-(*R*)-MA on the seed material at the onset of the process. The surrounding solution consequently enriches in nefi-(*S*)-MA. As CO_2 addition continues, supersaturation rapidly increases, leading to nucleation of nefi-(*S*)-MA and simultaneous rapid crystal growth of both enantiomers on the outer ring. As nefi-(*S*)-MA shows higher concentration in solution, faster crystallization of this enantiomer is then expected in the outer layers.

3.2.2.2. Decreasing initial solution concentration

In an attempt to reduce nucleation and crystal growth kinetics of the counter-enantiomer, Runs 19 and 20 were carried out decreasing the initial solution concentration. The initial reduced concentration should lead to a less supersaturated solution reaching the seed-material. Both runs indeed show a lower yield recovered on the cylinder (7.9 and 13.0% respectively), with increased *ee*'s (44 and 49% respectively). However, spontaneous crystallization of the counter-enantiomer still occurs, as no enantiopure material is obtained.

3.2.2.3. Decreasing seeding amount

Concurrently, attempts were made to reduce the quantity of enantiopure material used as seeds. Reducing the amount of seeds (first slightly reducing it with Run 17, then drastically reducing seeding amount with Run 18 vs Runs 10-11) does not seem to have any substantial impact on the crystallization kinetics, since comparable *ee* and yield were obtained. This aspect is advantageous for the economic evaluation of the process.

From Runs 7-20, it is clear that reproducibility is the main limitation of the GAS-induced preferential crystallization set-up. Ideally in preferential crystallization processes, nucleation of the counter-

enantiomer is avoided and/or rapid crystal growth of this latter reduced. In a classical-solution based batch process, multiple factors such as temperature, seed amount, stirring, and reactor set-up have an impact on the final result [6]. However, in our GAS set-up, additional factors, such as pressure evolution and CO_2 addition rate also impact this process, requiring careful control. Moreover, since CO_2 is continuously added and mixed with the solvent, the herein process is a non-equilibrium method in terms of fluid phases. Additionally, mixing is not an instantaneous phenomenon, and the compounds also have their own induction time (the time taken for the first nuclei to appear in response to the decrease in solubility [35]).

Importantly, however, our work highlights the robustness of the nefi-MA cocrystal-conglomerate system. Indeed, all experiments allowed the formation of the cocrystal, as confirmed by XRPD (Figure SI-3). Moreover, the feasibility of performing preferential crystallization through GAS is clearly highlighted. Based on our findings, future endeavors should orient towards an appropriate engineering of GAS-technology so that it is best-compatible with preferential crystallization. We initiated such development, investigating alternative set-ups of the cylinder.

3.2.3 *Steps towards an ideal preferential crystallization GAS set-up*

Our focus was placed on adapting the seeding configuration, aiming at achieving simultaneous crystallization of both enantiomers but in distinct areas of the reactor. By promoting their concurrent crystallization, we aimed at reducing the risk of spontaneous nucleation of the counter-enantiomer. We explored two alternatives to the seeding set-up used initially.

In a first alternative (Table 2, Runs 21-24), the seeded cylinder was covered on one side with nefi-(*R*)-MA seed material, and with nefi-(*S*)-MA on the other side (Figure 5). Using this set-up, we were able in all runs to control the preferential crystallization process by orienting it to a specific side of the seed-ring. In all cases, the supplementary material crystallizing on top of the seed is the nefi-MA cocrystal (Figure SI-4). Moreover, it is effectively enriched in the same enantiomer as the seed, with overall higher total *ee*'s compared to experiments where only a single enantiomer seed was used. Interestingly, with the solution being simultaneously depleted in both enantiomers, the material recovered elsewhere in the

reactor (stirrer, reactor, and outlet collector) remains a racemic mixture, contrasting with set-ups using only one type of seed material.

Further evidence of a more controlled preferential crystallization process is given by sampling across the crystalline layer deposited on the seeded cylinder (Figure 5, Table 4). In contrast to the single-enantiomer-seeded experiments discussed above (Table 3), here, the outer layer no longer exhibits an enrichment in the counter-enantiomer. Both outer and inner layers are now showing an excess in favor of the seed-enantiomer used. Moreover, there is very little difference in *ee*'s of the inner and outer layers (Table 4).

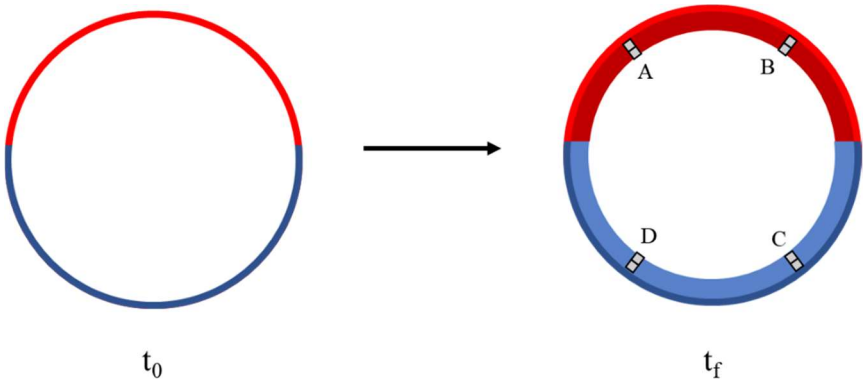

Figure 5. Cylinder seeded on one side with nefi-(*R*)-MA (dark blue) and the other with the nefi-(*S*)-MA (light red). Over time, a layer half enriched in nefi-(*R*)-MA (light blue) and half in nefi-(*S*)-MA (dark red), grows. The different samples taken are represented as grey squares.

Table 4. *c*HPLC results of the samples taken across the crystal material on the cylinder for Runs 21 and 23. Samples are recovered on the outer layer, and an inner layer closer to the seed material.

Run	*ee* cyl (%)	(*S*)-seeded half cylinder				(*R*)-seeded half cylinder			
		ee A		*ee* B		*ee* C		*ee* D	
		Outer	Inner	Outer	Inner	Outer	Inner	Outer	Inner
21	-37	-29	-40	-25	-25	---	---	---	---
	33	---	---	---	---	49	37	56	58
23	-65	-48	-66	-47	-57	---	---	---	---
	34	---	---	---	---	15	29	61	64

**ee* were determined by *c*HPLC, a positive result represents an enrichment in nefi-(*R*)-MA, and a negative result represents an enrichment in nefi-(*S*)-MA.

In a second alternative, seeding was performed by superposing two seeded cylinders (Table 2, Runs 25 and 26). In this configuration, the bottom cylinder was coated with nefi-(*R*)-MA, while the upper one was coated with nefi-(*S*)-MA (Figure 6).

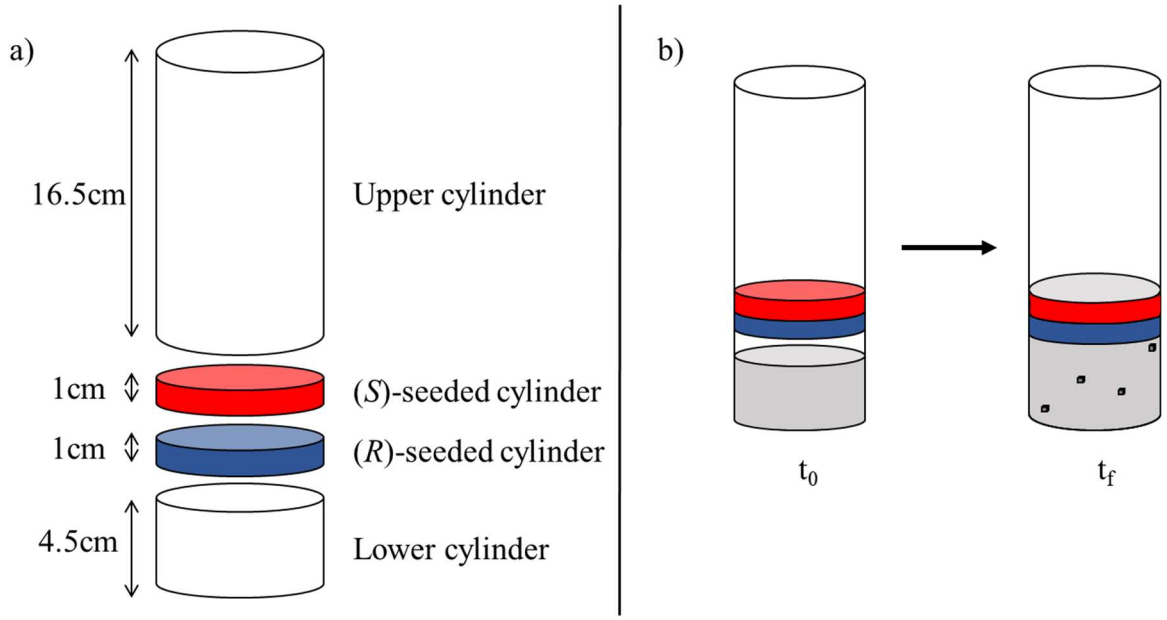

Figure 6. Preferential crystallization principle when superposing two seeded cylinders. a) Set-up of the cylinder with two different seed materials at a height of 4.5-5.5cm and 5.5-6.5cm, b) Evolution of the experiment over time.

Both pieces of the seed-cylinder show supplementary crystallized material, to be the nefi-MA cocrystal (Figure SI-5), enantioenriched according to the nature of seed material used, while powder recovered elsewhere in the reactor and on the stirrer is a racemic mixture. This indicates the success of this set-up in a controlled depletion of both enantiomers. The bottom-seeded cylinder – nefi-(*R*)-MA – shows less enrichment compared to the upper-seeded cylinder – nefi-(*S*)-MA – (*e.g.* Run 26 shows an *ee* of +21% for the lower cylinder, whereas an *ee* of -38% is obtained for the upper cylinder). This finding is coherent with a supersaturated solution reaching the first cylinder, where nefi-(*R*)-MA crystallizes more rapidly due to the *(R)*-seeding, albeit some of the nefi-(*S*)-MA also crystallizing concomitantly. The solution reaching the upper cylinder then shows a stronger depletion in nefi-(*R*)-MA. The upper (*S*)-

seeded cylinder, enhances the crystal growth of nefi-(*S*)-MA. Nucleation and growth kinetics of nefi-(*R*)-MA are less important, due to the lower supersaturation in (*R*)-cocrystal at this stage.

Looking at both configurations, it seems that parallel seeding, depleting the solution simultaneously of both enantiomers, is the preferred option. An optimization of this process can therefore be studied by playing on various parameters (concentration of the species, temperature at which the process takes place, height of seeding, CO_2 introduction rate, stirring rate…).

4. Conclusion

We here present the first occurrence of a GAS assisted preferential cocrystallization process.

Focusing on the nefiracetam-(*rac*)-mandelic acid system, we show that not only conglomerate formation can be induced in a GAS context, but that seeding can be used to orient the preferential crystallization of a given enantiomer in a specific area of the reactor. This is, to the best of our knowledge, the first occurrence of seed introduction in a supercritical reactor, in order to induce preferential crystal growth. Our results highlight that the absence of seed-material leads to concomitant crystallization of both enantiomers, whereas the use of enantiopure seeding, leads to material enriched in the same enantiomer. As GAS is an antisolvent process, rapid creation of supersaturation, however, always led to spontaneous nucleation of the counter-enantiomer as the process advanced (in the outer layers deposited). First steps, in achieving a higher degree of control over supersaturation, and the preferential crystallization process, highlighted the potential of using a parallel seeding set-up, with half of the seed-cylinder seeded with one enantiomer and the other half with the counter-enantiomer. This set-up, indeed allowed increased control over the process, with simultaneous depletion of both enantiomers, higher overall enrichment on both sides of the reactor, and less spontaneous nucleation of the counter-enantiomer in the outer deposited layers.

At this stage, we also emphasize the complexity of the process. Preferential crystallization is a kinetic process, requiring careful control over crystallization process parameters (concentration, temperature, seeding, …), which combined with the parameters of a GAS process (CO_2 addition rate, pressure control, mixing between CO_2 and the solvent, …) set future challenges for an optimal process design. We are

convinced that careful control of all these parameters, with an adapted reactor allowing for slower crystallization kinetics, will ultimately lead to a set-up allowing full resolution through CO_2 assisted preferential crystallization.

Author contributions

Conceptualization CHS, TL, PSP, YC, CB, MM; Formal analysis JdM, PL, LC, GW, CHS, TL PSP; Funding acquisition TL, PSP; Investigation JdM, PL, CHS; Methodology CHS PSP; Resources CHS, TL; Supervision CHS, TL, PSP; Roles/Writing - original draft JdM, TL, CHS, PSP; and Writing - review & editing JdM, CHS, TL, PSP, YC, CB, MM.

Declaration of competing interest

The authors declare the following financial interests/personal relationships which may be considered as potential competing interests: SUBRA PATERNAULT reports financial support was provided by French National Research Agency.

Data availability

Data will be made available on request.

Acknowledgements

This work was supported by the Fonds de la Recherche Scientifique – FNRS – *Financement Mobilité* under Grant n°40020442. The authors would also like to thank the FNRS (PDR T.0262.20) for funding. The financial support of french ANR Project CYPRES - ANR-18-CE07-0047 is greatly acknowledged.

Appendix A. Supplementary material

References

[1] H. Lorenz, A. Seidel-Morgenstern, Processes To Separate Enantiomers, Angew. Chem. Int. Ed. 53 (2014) 1218–1250. https://doi.org/10.1002/anie.201302823.

[2] J.I. Putman, D.W. Armstrong, Recent advances in the field of chiral crystallization, Chirality 34 (2022) 1338–1354. https://doi.org/10.1002/chir.23492.

[3] L.A. Nguyen, H. He, C. Pham-Huy, Chiral Drugs: An Overview, Int. J. Biomed. Sci. 2 (2006) 85–100.

[4] M. Kőrösi, J. Madarász, T. Sohajda, E. Székely, A fast, new method to enhance the enantiomeric purity of non-racemic mixtures: self-disproportionation of enantiomers in the gas antisolvent fractionation of chlorine-substituted mandelic acid derivatives, Tetrahedron: Asymmetry 28 (2017) 1568–1572. https://doi.org/10.1016/j.tetasy.2017.09.005.

[5] X. Buol, C. Caro Garrido, K. Robeyns, N. Tumanov, L. Collard, J. Wouters, T. Leyssens, Chiral Resolution of Mandelic Acid through Preferential Cocrystallization with Nefiracetam, Cryst. Growth Des. 20 (2020) 7979–7988. https://doi.org/10.1021/acs.cgd.0c01236.

[6] C. Rougeot, J.E. Hein, Application of Continuous Preferential Crystallization to Efficiently Access Enantiopure Chemicals, Org. Process Res. Dev. 19 (2015) 1809–1819. https://doi.org/10.1021/acs.oprd.5b00141.

[7] C. Brandel, Y. Amharar, J.M. Rollinger, U.J. Griesser, Y. Cartigny, S. Petit, G. Coquerel, Impact of Molecular Flexibility on Double Polymorphism, Solid Solutions and Chiral Discrimination during Crystallization of Diprophylline Enantiomers, Mol. Pharmaceutics 10 (2013) 3850–3861. https://doi.org/10.1021/mp400308u.

[8] W.W. Li, L. Spix, S.C.A. de Reus, H. Meekes, H.J.M. Kramer, E. Vlieg, J.H. ter Horst, Deracemization of a Racemic Compound via Its Conglomerate-Forming Salt Using Temperature Cycling, Cryst. Growth Des. 16 (2016) 5563–5570. https://doi.org/10.1021/acs.cgd.6b01034.

[9] K.K. Sarmah, T. Rajbongshi, A. Bhuyan, R. Thakuria, Effect of Solvent Polarity in Mechanochemistry: Preparation of Conglomerate vs. Racemate, Chem. Commun. 55 (2019) 10900–10903. https://doi.org/10.1039/C9CC05687D.

[10] S. Gonella, J. Mahieux, M. Sanselme, G. Coquerel, Spotting a Conglomerate Is Just Halfway to Achieving a Preparative Resolution by Preferential Crystallization, Org. Process Res. Dev. 16 (2012) 286–293. https://doi.org/10.1021/op200092f.

[11] F. Zhou, O. Shemchuk, M.D. Charpentier, C. Matheys, L. Collard, J.H. ter Horst, T. Leyssens, Simultaneous Chiral Resolution of Two Racemic Compounds by Preferential Cocrystallization**, Angewandte Chemie 60 (2021) 20426–20430. https://doi.org/10.1002/ange.202107804.

[12] L. Wang, N. Wang, J. Sui, S. Sun, Z. Feng, G. Li, H. Hao, L. Zhou, Case of Chiral Resolution through Converting Two Racemic Compounds into a Conglomerate, Cryst. Growth Des. 23 (2023) 5641–5650. https://doi.org/10.1021/acs.cgd.3c00311.

[13] L.C. Harfouche, C. Brandel, Y. Cartigny, S. Petit, G. Coquerel, Resolution by Preferential Crystallization of Proxyphylline by Using Its Salicylic Acid Monohydrate Co-Crystal, Chem Eng & Technol 43 (2020) 1093–1098. https://doi.org/10.1002/ceat.202000040.

[14] P. Rapeenun, C.J.J. Gerard, C. Pinètre, Y. Cartigny, P. Tinnemans, R. de Gelder, A.E. Flood, J.H. ter Horst, Searching for Conglomerate Cocrystals of the Racemic Compound Praziquantel, Cryst. Growth Des. 24 (2024) 480–490. https://doi.org/10.1021/acs.cgd.3c01158.

[15] M. Kőrösi, A. Sedon, K. Komka, T. Sohajda, E. Székely, Gas Antisolvent Fractionation: a New Method to Obtain Enantiopure Compounds, a Case Study on Mandelic Acid, Period. Polytech. Chem. Eng. 63 (2018) 130–137. https://doi.org/10.3311/PPch.11741.

[16] Ž. Knez, E. Markočič, M. Leitgeb, M. Primožič, M. Knez Hrnčič, M. Škerget, Industrial applications of supercritical fluids: A review, Energy 77 (2014) 235–243. https://doi.org/10.1016/j.energy.2014.07.044.

[17] J. Shi, X. Kang, L. Mao, Y. Jiang, S. Zhao, Y. Liu, B. Zhai, H. Jin, L. Guo, Supercritical CO2-applied equipment for chemical synthesis and transformation: Current status and perspectives, Chemical Engineering Journal 459 (2023) 141608. https://doi.org/10.1016/j.cej.2023.141608.

[18] Ž. Knez, M. Knez Hrnčič, M. Škerget, Particle Formation and Product Formulation Using Supercritical Fluids, Annu. Rev. Chem. Biomol. Eng. 6 (2015) 379–407. https://doi.org/10.1146/annurev-chembioeng-061114-123317.

[19] W. Leitner, Supercritical Carbon Dioxide as a Green Reaction Medium for Catalysis, Acc. Chem. Res. 35 (2002) 746–756. https://doi.org/10.1021/ar010070q.

[20] A. O'Sullivan, B. Long, V. Verma, K.M. Ryan, L. Padrela, Solid-state and particle size control of pharmaceutical cocrystals using atomization-based techniques, Int. J. Pharm. 621 (2022) 121798. https://doi.org/10.1016/j.ijpharm.2022.121798.

[21] E. Ramsey, Q. Sun, Z. Zhang, C. Zhang, W. Gou, Mini-Review: Green sustainable processes using supercritical fluid carbon dioxide, Journal of Environmental Sciences 21 (2009) 720–726. https://doi.org/10.1016/S1001-0742(08)62330-X.

[22] C. Neurohr, A.-L. Revelli, P. Billot, M. Marchivie, S. Lecomte, S. Laugier, S. Massip, P. Subra-Paternault, Naproxen–nicotinamide cocrystals produced by CO2 antisolvent, The Journal of Supercritical Fluids 83 (2013) 78–85. https://doi.org/10.1016/j.supflu.2013.07.008.

[23] F. Ercicek, C. Harscoat-Schiavo, P. Layrisse, M. Marchivie, Y. Cartigny, C. Brandel, T. Tassaing, M. Conrad, S. Marre, P. Subra-Paternault, Naproxen-bipyridine cocrystallization assisted by pressurized carbon dioxide, J. Supercrit. Fluids 200 (2023) 105976. https://doi.org/10.1016/j.supflu.2023.105976.

[24] G. Kotbantao, M. Charoenchaitrakool, Processing of ketoconazole–4-aminobenzoic acid cocrystals using dense CO 2 as an antisolvent, Journal of CO2 Utilization 17 (2017) 213–219. https://doi.org/10.1016/j.jcou.2016.12.007.

[25] F. Ercicek, M. Marchivie, L. Nimod, H. Cercel, C. Brandel, I. Ziri, Y. Cartigny, O. Monnier, S. Marre, D. Denux, P. Subra-Paternault, C. Harscoat-Schiavo, Unraveling a Unique Metastable phase of a Proxyphylline Co-crystal exclusively produced by Compressed Carbon Dioxide, Unpublished results

[26] D. Varga, G. Bánsághi, J.A.M. Pérez, S. Miskolczi, L. Hegedűs, B. Simándi, E. Székely, Chiral Resolution of Racemic Cyclopropanecarboxylic Acids in Supercritical Carbon Dioxide, Chem Eng & Technol 37 (2014) 1885–1890. https://doi.org/10.1002/ceat.201300720.

[27] G. Bánsághi, E. Székely, D.M. Sevillano, Z. Juvancz, B. Simándi, Diastereomer salt formation of ibuprofen in supercritical carbon dioxide, The Journal of Supercritical Fluids 69 (2012) 113–116. https://doi.org/10.1016/j.supflu.2012.05.016.

[28] L. Lőrincz, G. Bánsághi, M. Zsemberi, S. de Simón Brezmes, I.M. Szilágyi, J. Madarász, T. Sohajda, E. Székely, Diastereomeric salt precipitation based resolution of ibuprofen by gas

antisolvent method, The Journal of Supercritical Fluids 118 (2016) 48–53. https://doi.org/10.1016/j.supflu.2016.07.021.

[29] A. Zodge, M. Kőrösi, J. Madarász, I.M. Szilágyi, E. Varga, E. Székely, Gas Antisolvent Fractionation: A New Approach for the Optical Resolution of 4-chloromandelic Acid, Period. Polytech. Chem. Eng. 63 (2019) 303–311. https://doi.org/10.3311/PPch.12910.

[30] P.-L. Wang, H.-B. Wang, W.-L. Ding, Z.-Q. Liu, Z.-T. Xing, *N* -(2,6-Dimethylphenyl)-2-(2-oxo-1-pyrrolidin-1-yl)acetamide, Acta Crystallogr E Struct Rep Online 62 (2006) o3838–o3839. https://doi.org/10.1107/S1600536806031370.

[31] T.S. Cameron, M. Duffin, DL-mandelic acid, J Mol Biol 3 (1974) 539-541. https://doi.org/10.1016/0022-2836(75)90229-6.

[32] A.O. Patil, W.T. Pennington, I.C. Paul, D.Y. Curtin, C.E. Dykstra, Reactions of crystalline (R)-(-)- and (S)-(+)-mandelic acid with amines. Crystal structure and dipole moment of (S)-mandelic acid. A method of determining absolute configuration of chiral crystals, J. Am. Chem. Soc. 109 (1987) 1529–1535. https://doi.org/10.1021/ja00239a037.

[33] C. Harscoat-Schiavo, C. Neurohr, S. Lecomte, M. Marchivie, P. Subra-Paternault, Influence of isomerism on recrystallization and cocrystallization induced by CO_2 as an antisolvent, CrystEngComm 17 (2015) 5410–5421. https://doi.org/10.1039/C5CE00753D.

[34] A. Erriguible, C. Neurohr, A.-L. Revelli, S. Laugier, G. Fevotte, P. Subra-Paternault, Cocrystallization induced by compressed CO2 as antisolvent: Simulation of a batch process for the estimation of nucleation and growth parameters, J. Supercrit. Fluids 98 (2015) 194–203. https://doi.org/10.1016/j.supflu.2014.12.013.

[35] S.A. Kulkarni, S.S. Kadam, H. Meekes, A.I. Stankiewicz, J.H. ter Horst, Crystal Nucleation Kinetics from Induction Times and Metastable Zone Widths, Cryst. Growth Des. 13 (2013) 2435–2440. https://doi.org/10.1021/cg400139t.